

Dynamical Crossover from Markovian to Non-Markovian dynamics in the strong coupling regime

Md. Manirul Ali^{1,*} and Chandrashekar Radhakrishnan^{2,1,†}

¹*Centre for Quantum Science and Technology, Chennai Institute of Technology, Chennai 600069, India*

²*Centre for Quantum Information, Communication and Computing,
Indian Institute of Technology Madras, Chennai 600036, India*

(Dated: January 20, 2022)

The transient dynamics of quantum coherence of Gaussian states are investigated. The state is coupled to an external environment which can be described by a Fano-Anderson type Hamiltonian. Solving the quantum Langevin equation, we obtain the Greens functions which are used to compute the time evolved first and second moments of the quadrature operators. From the quadrature operator moments, we construct the covariance matrix which is used to measure the coherence in the system. The coherence is measured using the relative entropy of coherence measure. We consider three different classes of spectral densities in our analysis *viz*, the Ohmic, the sub-Ohmic, and the super-Ohmic densities. In our work, we study the dynamics of the coherent state, squeezed state, and displaced squeezed state. For all these states we observe that when the coupling with the system and the environment is weak, the coherence monotonically decreases and eventually vanishes in a long time. Thus all the states exhibit Markovian evolution in the weak coupling limit. In the strong coupling limit, the dynamics for the initial period is Markovian and after a certain period, it becomes non-Markovian where we observe an environmental backaction on the system. Thus in the strong coupling limit, we observe a dynamical crossover from Markovian nature to non-Markovian behavior. This crossover is very abrupt under some environmental conditions and for some parameters of the quantum state. Using a quantum master equation approach we verify the crossover from the dynamics of the dissipation and fluctuation parameters and the results endorse those obtained from coherence dynamics.

I. INTRODUCTION

Quantum coherence arises due to the superposition principle and is an essential property of quantum systems. Basic features of coherence were well studied through [1], where they were investigated in the context of quantum optics. But these studies have focused only on the detection of quantum coherence while a method to estimate coherence was not available. A procedure to measure coherence using a quantum information theoretic framework was introduced by Baumgratz et. al. in Ref. [2]. This method is used to estimate the coherence of finite dimensional systems. This led to some fundamental results in the field of resource theory of quantum coherence [3–7]. Subsequently quantum coherence has been studied in the contexts, where the system is either in a non-inertial frame of reference [8, 9] or where the system is in contact with an external environment [10–13]. But most of these investigations have been carried out on quantum systems with finite number of degrees of freedom like qubits.

Quantum communication requires a quantum description of the interaction and propagation of electromagnetic waves. An infinite number of degrees of freedom with continuous spectrum is needed to describe the electromagnetic waves. Hence from both theoretical and experimental perspective, continuous variable (CV) states [14–17] of

infinite dimensional systems are very important. Continuous variable systems constitute an extremely powerful resource to quantum information processing. One particular class of continuous variable states is the Gaussian states [16–18] for which the quantum state has a representation in terms of Gaussian functions. To a first approximation, the ground states of the thermal states of a quantum system is a Gaussian state. Similarly there are dynamical operations in which quantum states are transformed to another Gaussian states and these are referred to as Gaussian operations. The Gaussian operations are linear in nature and any nonlinear operation can be approximated to a Gaussian operation to a satisfactory level of accuracy. In light of these reasons, the Gaussian states occupy a special place in the study of continuous variable systems. The first quantum resource to be studied extensively in a Gaussian state is its entanglement. Since a covariance matrix along with the displacement vectors completely characterizes a Gaussian state, the entanglement can be quantified using a covariance matrix based approach. To measure the quantum coherence of Gaussian states a measure based on relative entropy, using covariance matrix and displacement vectors was introduced in Ref. [19]. The fundamental postulates of (i) positivity (ii) monotonicity and (iii) convexity were verified for this relative entropy measure.

In most of the investigations on discrete and continuous variable systems, we do not consider the effect of the external environment on the system. But in reality the quantum systems are exposed to an environment, which acts as a bath and affects the characteristics of the system by

* manirul@citchennai.net

† chandrashekar10@gmail.com

constantly interacting with it. To understand the effects of the environment and incorporate them in the characterization of the quantum resources, we take an open quantum system approach. Here we model the environment as a quantum many-body object which is coupled to the system. Based on the strength of the coupling and the other characteristics of the system and the environment, there is a dynamical change in the quantum resource. Depending on the bath spectrum and whether the system is weakly or strongly coupled to the environment, the system can exhibit a Markovian or non-Markovian dynamics [20, 21]. A quantum resource can completely disappear and then reappear a phenomenon known as revival. These features are dependent not only on the initial properties of the bath and the system but also on how they are coupled to each other. Understanding this dynamical change is essential to the fabrication of quantum devices [22–29]. It provides us a clear idea of the operational time of the quantum devices, i.e., the time within which the quantum operations have to be completed before the quantum resources vanish. The time evolution of the entanglement of finite dimensional systems has been investigated in a very detailed manner and some unique features like sudden death of entanglement [30–32] and entanglement revival [33–36] due to environmental back action have been observed. For continuous variable systems, investigations on the dynamics of entanglement have been done [37–39]. An open quantum system study of coherence has been carried out using an atom-field interaction model [11] and a central spin model [12]. The dynamics of coherence and its distribution was extensively investigated for the different bipartite and tripartite states. But both these investigations were carried out on finite dimensional system. For the continuous variable systems, the quantum coherence dynamics has not been investigated so far. In this work we investigate the dynamics of coherence of a single mode Gaussian states *viz* the coherent state, the squeezed state and the displaced squeezed state.

The plan of the manuscript is as follows: In Sec. II we give a brief introduction to the continuous variable quantum state and explain the Gaussian states in detail. Also we describe the covariance matrix based coherence measure introduced in Ref. [19]. The description of the Gaussian state in contact with a non-Markovian environment is described in Sec. III. For the single mode coherent states the dynamics of quantum coherence is discussed in Sec. IV. Next we study the effect of non-Markovian environment on squeezed states in Sec. V. An analysis of coherence in the single mode displaced squeezed state is shown in Sec. VI. Finally in Sec. VII, we investigate the crossover from Markovian to non-Markovian dynamics. We present our conclusions in Sec. VIII.

II. GAUSSIAN STATES AND QUANTIFICATION OF COHERENCE

A. Gaussian states

A continuous variable quantum system [14, 15] has an infinite dimensional Hilbert space in which observables have a continuous eigenspectrum. An example of a continuous-variable system is the electromagnetic field in which the quantized radiation modes are represented by the bosonic modes. The tensor product Hilbert space corresponding to these modes is $\otimes_{k=1}^n H_k$, where ‘ n ’ is the number of bosonic modes. For a given mode ‘ k ’ of the bosonic field, the operators a_k^\dagger and a_k are the corresponding creation and annihilation operators. Apart from the bosonic field operators, the continuous-variable system can also be described using the quadrature operators $\{x_k, p_k\}$. The quadrature field operators can be arranged in the form of a $2n$ -dimensional vector as $\boldsymbol{\xi} = (x_1, p_1, \dots, x_n, p_n)$. Here the $2n$ -dimensional vectors $\boldsymbol{\xi}$ contains the quadrature pairs of all the n modes. In terms of the bosonic field operators, the quadrature operators $\{x_k, p_k\}$ are expressed as

$$x_k = (a_k + a_k^\dagger), \quad p_k = -i(a_k - a_k^\dagger),$$

and they are canonically conjugate to each other. These quadrature field operators act similar to the canonically conjugate position and momentum operators of a harmonic oscillator.

In the present work we study a single-mode continuous variable system. The two quadrature operators corresponding to the single mode continuous variable system are $\xi_1 = x = (a + a^\dagger)$ and $\xi_2 = p = -i(a - a^\dagger)$ and the 2D-vector $\boldsymbol{\xi} = \{\xi_1, \xi_2\}$. The quadrature operators satisfy the canonical commutation relations $[\xi_i, \xi_j] = 2i\Omega_{ij}$, where Ω_{ij} are the elements of the matrix

$$\boldsymbol{\Omega} = \begin{pmatrix} 0 & 1 \\ -1 & 0 \end{pmatrix}. \quad (2.1)$$

In particular, we study the coherence dynamics of the Gaussian states. The Gaussian states [16, 18] are defined as the states with Gaussian Wigner function. For a Gaussian state, the Wigner quasiprobability distribution is

$$W(\boldsymbol{\xi}) = \frac{1}{2\pi\sqrt{\det \mathbf{V}}} \exp \left\{ -\frac{1}{2}(\boldsymbol{\xi} - \bar{\boldsymbol{\xi}}) \cdot \mathbf{V}^{-1}(\boldsymbol{\xi} - \bar{\boldsymbol{\xi}})^T \right\}$$

A Gaussian state is completely characterized by the first and the second moments of the quadrature field operators. Here the vector of the first moments $\bar{\boldsymbol{\xi}} = (\langle \xi_1 \rangle, \langle \xi_2 \rangle)$ and the covariance matrix \mathbf{V}

$$V_{ij} = \langle \{\Delta \xi_i, \Delta \xi_j\} \rangle = \text{Tr}(\{\Delta \xi_i, \Delta \xi_j\} \rho), \quad (2.2)$$

where $\Delta \xi_i = \xi_i - \langle \xi_i \rangle$ is the fluctuation operator and $\{\Delta \xi_i, \Delta \xi_j\} = (\Delta \xi_i \Delta \xi_j + \Delta \xi_j \Delta \xi_i)/2$. For the single mode quantum system under consideration, the matrix elements

of the covariance matrix are

$$V_{ii} = \langle \xi_i^2 \rangle - \langle \xi_i \rangle^2, \quad (2.3)$$

$$V_{ij} = \frac{1}{2} \langle \xi_i \xi_j + \xi_j \xi_i \rangle - \langle \xi_i \rangle \langle \xi_j \rangle. \quad (2.4)$$

To reflect the positivity of the density matrix, the covariance matrix has to satisfy the uncertainty relation [40] $V + i\Omega \geq 0$.

B. Measurement of Coherence

The quantum coherence of a qubit system is measured as follows: First we define the set of incoherent states \mathcal{I} , i.e., the states with zero coherence. Next we use a suitable distance measure to find the distance between the arbitrary density matrix and the closest incoherent states. In Ref. [2], the authors used the relative entropy measure to quantify the amount of coherence in the system. In general the relative entropy distance between two density matrices is

$$D(\rho) = \min_{\sigma} S(\rho||\sigma) = \min_{\sigma} \text{Tr}(\rho \log_2 \rho - \rho \log_2 \sigma), \quad (2.5)$$

where ρ is the given quantum state and σ is the reference state. Using this formulation we can find the coherence in the system by assuming the reference state to be the incoherent state. It has been proved that for the relative entropy of coherence, the closest incoherent state is $\rho_d = \sum_n \rho_{nn} |n\rangle\langle n|$, which is the diagonal state of the density matrix. Hence it is not necessary to perform the minimization to determine the quantum coherence. The relative entropy measure reads:

$$C(\rho) = S(\rho||\rho_d) = S(\rho_d) - S(\rho), \quad (2.6)$$

where $S(\rho) = -\text{tr}(\rho \log_2 \rho)$ is the vonNeumann entropy of the system. So far, the relative entropy of coherence is the most widely used measure. The quantum coherence of continuous variable system was first investigated in [41]. Here the authors used a relative entropy based quantifier of coherence by considering the density matrix ρ in the Fock basis. While this method is a valid process to quantify coherence, it does not give a closed form expression for general Gaussian states. Alternatively in Ref. [19], the coherence measure for a one-mode Gaussian state ρ was defined as

$$C(\rho) = \inf_{\delta} S(\rho||\delta). \quad (2.7)$$

Here $S(\rho||\delta)$ is the relative entropy measure with δ being an incoherent Gaussian state and the infimum runs over all incoherent Gaussian states. Also, it was proved that a one mode Gaussian state is incoherent if and only if it is a thermal state. Hence for a Gaussian state, the minimization is achieved for thermal states of the form

$$\rho_d = \bar{\rho} = \sum_{n=0}^{\infty} \frac{\bar{n}^n}{(1 + \bar{n})^{n+1}} |n\rangle\langle n|, \quad (2.8)$$

where $\bar{n} = \text{Tr}[a^\dagger a \bar{\rho}]$ is the mean number. For the Gaussian states, the entropy of a given state ρ can be written as

$$S(\rho) = \frac{\nu + 1}{2} \log_2 \frac{\nu + 1}{2} - \frac{\nu - 1}{2} \log_2 \frac{\nu - 1}{2}, \quad (2.9)$$

where $\nu = \sqrt{\det V}$. Based on these expressions, the relative entropy based coherence measure for the Gaussian states is

$$C(\rho) = S(\rho||\bar{\rho}) = \text{Tr}(\rho \log_2 \rho - \rho \log_2 \bar{\rho}) \quad (2.10)$$

$$= \frac{\nu - 1}{2} \log_2 \frac{\nu - 1}{2} - \frac{\nu + 1}{2} \log_2 \frac{\nu + 1}{2} + (\bar{n} + 1) \log_2 (\bar{n} + 1) - \bar{n} \log_2 \bar{n}. \quad (2.11)$$

Hence the quantum coherence of a Gaussian state is completely determined by the determinant of the covariance matrix and the mean number \bar{n} associated with the Gaussian state. But this measure can be used to compute coherence of only Gaussian states. It is important to note that when the system-environment interaction Hamiltonian is bilinear in the creation and annihilation operators, the Gaussian nature of the quantum states is preserved during the time evolution [18, 42].

III. SINGLE MODE GAUSSIAN STATES IN A NON-MARKOVIAN ENVIRONMENT

A study of the dynamics of quantum coherence of qubit systems have been investigated both theoretically [10–12] and experimentally [13, 43]. On the theoretical side, the dynamics was characterized in atomic systems and spin systems for both Markovian and non-Markovian environments. Experimentally in [13, 43], the dynamics of coherence, entanglement and mutual information were compared in qubit system. In the present work we consider a continuous variable system consisting of a single bosonic mode of frequency ω_0 coupled to a general non-Markovian environment [44–48] at finite temperature. The single bosonic mode can be either a quantum optical field, a superconducting resonator or a nano-mechanical oscillator. A structured bosonic reservoir with a collection of infinite modes of varying frequencies can describe a general non-Markovian environment. The entire system comprising of the single bosonic mode and the reservoir can be described by the Fano-Anderson Hamiltonian [49, 50]. This Hamiltonian was introduced in the context of atomic [50] and condensed matter physics [49] and has been used to study several different models. The Fano-Anderson Hamiltonian of the system and bath combination is:

$$H = \hbar\omega_0 a^\dagger a + \hbar \sum_k \omega_k b_k^\dagger b_k + \hbar \sum_k \left(\mathcal{V}_k a^\dagger b_k + \mathcal{V}_k^* b_k^\dagger a \right), \quad (3.1)$$

where ω_0 is the system frequency and a^\dagger (a) is the creation (annihilation) operator corresponding to the bosonic mode (system) and b_k^\dagger (b_k) is the creation (annihilation) operator

of the k^{th} mode of the bosonic reservoir with frequency ω_k . The factor \mathcal{V}_k represents the coupling strength between the system and the environment.

The dynamics of the single mode system and the environment is solved using the Heisenberg equation of motion approach. The time evolution of the bosonic field operator and the environment operators reads:

$$a(t) = e^{\frac{iHt}{\hbar}} a e^{-\frac{iHt}{\hbar}}, \quad b_k(t) = e^{\frac{iHt}{\hbar}} b_k e^{-\frac{iHt}{\hbar}}. \quad (3.2)$$

In the Heisenberg picture, these operators satisfy the following equations of motion,

$$\frac{d}{dt}a(t) = -\frac{i}{\hbar} [a(t), H] = -i\omega_0 a(t) - i \sum_k \mathcal{V}_k b_k(t), \quad (3.3)$$

$$\frac{d}{dt}b_k(t) = -\frac{i}{\hbar} [b_k(t), H] = -i\omega_k b_k(t) - i\mathcal{V}_k^* a(t). \quad (3.4)$$

Solving for Eqn. (3.4) for b_k we get the solution

$$b_k(t) = b_k(0)e^{-i\omega_k t} - i\mathcal{V}_k^* \int_0^t d\tau a(\tau) e^{-i\omega_k(t-\tau)}. \quad (3.5)$$

Substituting Eq. (3.5) in (3.3) we arrive at the following quantum Langevin equation [51]

$$\dot{a}(t) + i\omega_0 a(t) + \int_0^t d\tau g(t, \tau) a(\tau) = -i \sum_k \mathcal{V}_k b_k(0) e^{-i\omega_k t}. \quad (3.6)$$

Here the integral kernel $g(t, \tau) = \sum_k |\mathcal{V}_k|^2 e^{-i\omega_k(t-\tau)}$ characterizes the non-Markovian memory effects between the system and the environment. For the continuous environment spectrum $g(t, \tau) = \int_0^\infty d\omega J(\omega) e^{-i\omega(t-\tau)}$, where $J(\omega) = \varrho(\omega) |\mathcal{V}(\omega)|^2$ is the spectral density which characterizes all the non-Markovian memory of the environment on the system. Here $\varrho(\omega)$ being the density of states of the environment and ω is the continuously varying frequency of the bath. Due to the linearity of Eq. (3.6) the time evolved bosonic operator $a(t)$ can be expressed [52] in terms of the initial field operators $a(0)$ and $b_k(0)$ of the system and the environment as

$$a(t) = u(t)a(0) + f(t). \quad (3.7)$$

The time-dependent coefficient $u(t)$ and noise operator $f(t)$ are determined by the quantum Langevin equation, and they satisfy the two integrodifferential equations given below:

$$\frac{d}{dt}u(t) = -i\omega_0 u(t) - \int_0^t d\tau g(t, \tau) u(\tau), \quad (3.8)$$

$$\begin{aligned} \frac{d}{dt}f(t) = & -i\omega_0 f(t) - \int_0^t d\tau g(t, \tau) f(\tau) \\ & - i \sum_k \mathcal{V}_k b_k(0) e^{-i\omega_k t}. \end{aligned} \quad (3.9)$$

To determine $u(t)$ we solve Eqn. (3.8) numerically with the initial condition $u(0) = 1$. Here the solution for the noise

operator obtained using the initial condition $f(0) = 0$ is

$$f(t) = -i \sum_k \mathcal{V}_k b_k(0) \int_0^t d\tau e^{-i\omega_k \tau} u(t, \tau). \quad (3.10)$$

The nonequilibrium thermal fluctuation can be evaluated using the quantity

$$\langle f^\dagger(t) f(t) \rangle = v(t) = \int_0^t d\tau_1 \int_0^{\tau_1} d\tau_2 u(t, \tau_1) \tilde{g}(\tau_1, \tau_2) u^*(t', \tau_2), \quad (3.11)$$

where we consider the initial state of the total system to be $\rho_{tot}(0) = \rho_S(0) \otimes \rho_E(0)$. Here the initial environment state $\rho_E(0) = \exp(-\beta H_E) / \text{Tr}[\exp(-\beta H_E)]$ is the thermal state for the Hamiltonian $H_E = \sum_k \hbar \omega_k b_k^\dagger b_k$, where $\beta = 1/k_B T$ is the inverse temperature and k_B is the Boltzmann constant.

When the environment has a continuous spectrum, the time correlation function reads:

$$\tilde{g}(\tau_1, \tau_2) = \int_0^\infty d\omega J(\omega) \bar{n}(\omega) e^{-i\omega(\tau_1 - \tau_2)}, \quad (3.12)$$

where $\bar{n}(\omega) = 1/(e^{\hbar\omega/k_B T} - 1)$ is the initial particle number distribution of the bosonic environment. From the Eqs. (3.7) to (3.11), one can obtain the time-dependent average values of the system operators as follows:

$$\langle a(t) \rangle = u(t) \langle a(0) \rangle, \quad \langle a^\dagger(t) \rangle = u^*(t) \langle a^\dagger(0) \rangle, \quad (3.13)$$

$$\langle a(t) a(t) \rangle = (u(t))^2 \langle a(0) a(0) \rangle, \quad (3.14)$$

$$\langle a^\dagger(t) a^\dagger(t) \rangle = (u^*(t))^2 \langle a^\dagger(0) a^\dagger(0) \rangle, \quad (3.15)$$

$$\langle a^\dagger(t) a(t) \rangle = |u(t)|^2 \langle a^\dagger(0) a(0) \rangle + v(t). \quad (3.16)$$

Here we consider $\langle f(t) \rangle = \langle f^\dagger(t) \rangle = 0$ and also $\langle f(t) f(t) \rangle = \langle f^\dagger(t) f^\dagger(t) \rangle = 0$, since the reservoir is initially in a thermal state uncorrelated to the system. Using the time-dependent average values in Eqs (3.13) - (3.16), we can evaluate the time evolved first and second moments of the quadrature operators namely, $\langle \xi_1(t) \rangle$, $\langle \xi_2(t) \rangle$, $\langle \xi_1^2(t) \rangle$, $\langle \xi_2^2(t) \rangle$, $\langle \xi_1(t) \xi_2(t) \rangle$, and $\langle \xi_2(t) \xi_1(t) \rangle$. The elements of the time evolved covariance matrix are

$$\begin{aligned} V_{11} = & 1 + 2v(t) + 2|u(t)|^2 \text{Cov}(a^\dagger(0), a(0)) \\ & + (u(t))^2 \text{Var}(a(0)) + (u^*(t))^2 \text{Var}(a^\dagger(0)), \end{aligned} \quad (3.17)$$

$$\begin{aligned} V_{22} = & 1 + 2v(t) + 2|u(t)|^2 \text{Cov}(a^\dagger(0), a(0)) \\ & - (u(t))^2 \text{Var}(a(0)) - (u^*(t))^2 \text{Var}(a^\dagger(0)), \end{aligned} \quad (3.18)$$

$$V_{12} = i(u^*(t))^2 \text{Var}(a^\dagger(0)) - i((u(t))^2 \text{Var}(a(0))). \quad (3.19)$$

where $\text{Cov}(a, b) = \langle ab \rangle - \langle a \rangle \langle b \rangle$ and $\text{Var}(a) = \text{Cov}(a, a)$ and $V_{12} = V_{21}$ due to the symmetry of the covariance matrix.

Once the initial state and the bath parameters are known, the time evolved covariance matrix elements are completely determined using the nonequilibrium Green's

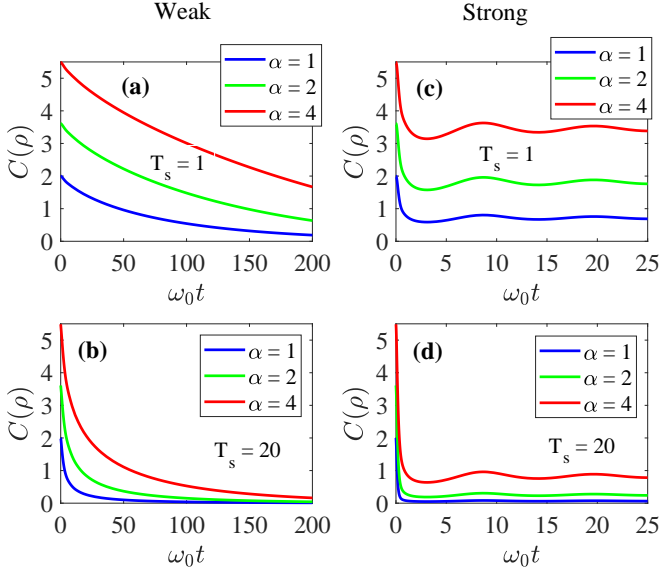


Figure 1: The time evolution of quantum coherence of a coherent state with parameter α in contact with a Ohmic bath is shown for weakly coupled systems ($\eta = 0.01 \eta_c$) in (a) at low temperature $T_s = 1$, (b) at high temperature $T_s = 20$ and for the strongly coupled systems ($\eta = 2.0 \eta_c$) in (c) at low temperature $T_s = 1$, (d) at high temperature $T_s = 20$. We use the cut-off frequency $\omega_c = 5.0 \omega_0$.

function $u(t)$ and $v(t)$. To calculate the Green's function we need to specify the spectral density $J(\omega)$ of the environment. In our work we consider a Ohmic-type spectral density which can simulate a large class of thermal baths [53]

$$J(\omega) = \eta \omega \left(\frac{\omega}{\omega_c} \right)^{s-1} e^{-\omega/\omega_c}, \quad (3.20)$$

where η is the coupling strength between the system and the environment and ω_c is the frequency cut-off of the environmental spectra. A localized mode is generated when the system-environment coupling approaches a critical value $\eta_c = \omega_0/(\omega_c \Gamma(s))$ where $\Gamma(s)$ is the Gamma function. Depending on the value of s , the environment is classified as Ohmic for $s = 1$, sub-Ohmic for $s < 1$ and super-Ohmic for $s > 1$. Throughout our work we use a scaled temperature $T_s = k_B T / \hbar \omega_0$, where ω_0 is the system frequency. The coherence dynamics for different environmental conditions, and various system-environment couplings is studied for pure Gaussian states through our work. Since the Hamiltonian under consideration (3.1) is bilinear in the creation and annihilation operators, during evolution, the Gaussian states preserve their form and remain Gaussian.

IV. QUANTUM COHERENCE DYNAMICS OF COHERENT STATES IN A NON-MARKOVIAN ENVIRONMENT

Glauber [1] defined a coherent state $|\alpha\rangle$ as the eigenstate of the annihilation operator a with eigenvalue $\alpha \in \mathbb{C}$. We can generate the coherent state from the ground state $|0\rangle$ of an oscillator through the action of the displacement operator $D(\alpha) = \exp(\alpha a^\dagger - \alpha^* a)$, where a^\dagger and a are the annihilation and creation operators of the standard harmonic oscillator. In the number basis, the coherent states can be expressed as

$$|\alpha\rangle = \exp\left(-\frac{1}{2}|\alpha|^2\right) \sum_{n=0}^{\infty} \frac{\alpha^n}{\sqrt{n!}} |n\rangle. \quad (4.1)$$

where $|n\rangle$ is the oscillator number basis. The coherent states are Gaussian wavepackets which does not spread and has minimal uncertainty. Thus for a free classical mode, the closest quantum analogue is the coherent state. Hence the coherent state is very useful in quantum optics especially to study the state of the quantized electromagnetic field. The time evolution of the quantum coherence of a coherent state subjected to a spectral density of the form given in Eq. (3.20) is reported in this section. Depending on the value of the parameter s , the environments are classified as Ohmic $s = 1$, sub-Ohmic $s < 1$ and super-Ohmic $s > 1$.

Ohmic bath ($s=1$):

The time dynamics of quantum coherence of a coherent state for a Ohmic bath with spectral density $J(\omega) = \eta \omega \exp(-\omega/\omega_c)$ is shown in Fig. 1. From the plots Figs 1(a) - (d) we find that higher the value of the coherent state parameter ' α ' higher the initial amount of coherence and also the value at a given time. In Fig 1(a) and 1(b) the time variation of coherence, when the system is weakly coupled to the environment i.e., $\eta = 0.01 \eta_c$ is shown. Particularly in Fig. 1(a) we look at the low temperature limit and in Fig. 1(b), the high temperature regime of the coherence dynamics. From both these plots we find that quantum coherence decreases monotonically with time. But it falls faster at higher temperature because apart from the environmental effects, the thermal effects also contribute to the system decoherence. The dynamics of coherence when the system is strongly coupled to the environment i.e., for $\eta = 2.0 \eta_c$ is shown in Fig. 1(c) and 1(d). Here we can see that the coherence initially decreases monotonically and then there is an oscillatory phase. This oscillatory phase is because of the environmental back action due to the non-Markovian nature of the bath. For lower temperatures as shown in Fig. 1(c), the coherence saturates at a higher value compared to the high temperature limit given in Fig. 1(d).

Sub-Ohmic bath ($s=1/2$):

To investigate the coherence dynamics in the sub-Ohmic region we consider $s = 1/2$ in Eq. (3.20). The corresponding spectral density reads $J(\omega) = \eta \sqrt{\omega \omega_c} \exp(-\omega/\omega_c)$. The results corresponding to this analysis is presented

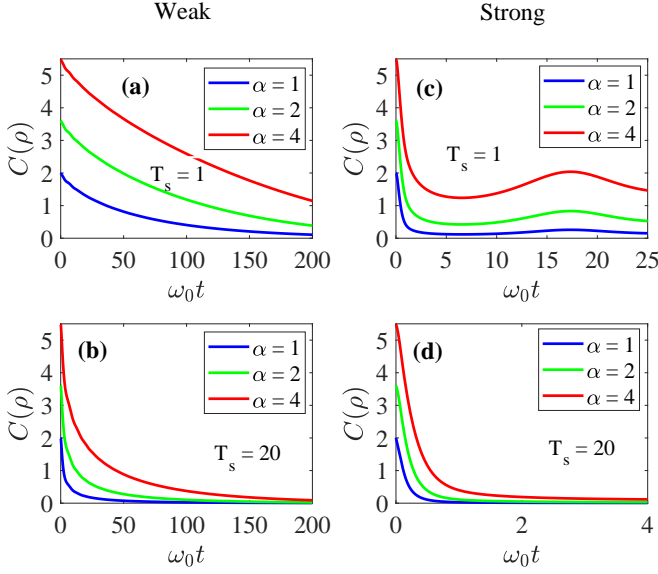


Figure 2: The coherence dynamics of a coherent mode with parameter r in contact with sub-Ohmic bath is studied for weakly coupled systems ($\eta = 0.01 \eta_c$) in (a) low temperature $T_s = 1$, (b) high temperature $T_s = 20$. For the strongly coupled systems ($\eta = 2.0 \eta_c$) the plots are (c) at low temperature $T_s = 1$ and (d) at high temperature $T_s = 20$. We use the cut-off frequency $\omega_c = 5.0 \omega_0$.

in Fig. 2. The time variation of coherence for the weak coupling limit with $\eta = 0.01 \eta_c$ is given in Fig. 2 (a) and (b). In Fig. 2 (a) the low temperature limit is analyzed and we find that the coherence decreases monotonically with time. At higher temperatures also, coherence decreases monotonically but the fall is much faster as seen in Fig. 2 (b). This faster fall is because at high temperatures apart from the dissipation, the thermal fluctuations also cause a decoherence in the system. The coherence dynamics when the system is strongly coupled to the environment $\eta = 2.0 \eta_c$ is presented in Fig. 2 (c) and (d) corresponding to the low and high temperature cases respectively. In the low temperature case illustrated in Fig. 2 (c), we find a revival of coherence due to the non-Markovian effects of the bath. Such a coherence revival is not observed in the high temperature limit even in the strong coupling case. This is because the temperature affects the environmental back action on the system, a feature which has also been observed in Ref. [1].

Super-Ohmic bath ($s=3$):

For the super-Ohmic bath we consider $s = 3$ to investigate the dynamics of coherence. The spectral density in this case reads $J(\omega) = \eta \omega_c (\omega/\omega_c)^3 \exp(-\omega/\omega_c)$. The coherence evolution in this case is described through the plots in Fig. 3 (a) to (d) considering different coupling strengths and different temperatures. In Fig. 3 (a) and (b) we analyze the coherence variation in the weak coupling limit when $\eta = 0.01 \eta_c$. Here we can see that the coherence decreases monotonically both in the low and high temperature limits. Due to temperature dependent

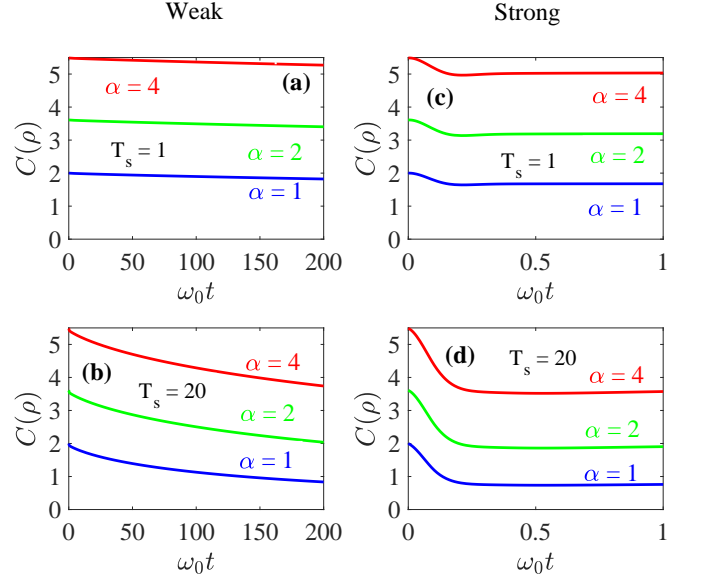


Figure 3: A coherent mode in contact with a super-Ohmic bath is studied for weakly interacting systems ($\eta = 0.01 \eta_c$) for (a) $T_s = 1$ and (b) $T_s = 20$ and also for strongly interacting systems ($\eta = 2.0 \eta_c$) with (c) $T_s = 1$ and (d) $T_s = 20$. The cut-off frequency used is $\omega_c = 5.0 \omega_0$.

decoherence effects, the rate of decrease is higher in Fig 3 (b). The nature of coherence variation in the strong coupling limit ($\eta = 2.0 \eta_c$) is examined in Fig. 3 (c) and (d) respectively. In both these cases we see that the coherence decreases initially and then saturates at a finite value a phenomenon known as coherence freezing. But the value at which coherence freezes is different in Fig. 3 (c) and Fig. 3 (d) and is also dependent on the parameter α . For a higher α , the coherence freezes at a higher value. The general decrease in coherence is due to the environmental effects. For the same environment at different temperatures, the system experiences temperature dependent decoherence effects.

V. NON-MARKOVIAN DYNAMICS OF SQUEEZED STATES

A squeezed state has a minimum value for the product of the dispersion of the position and momentum operators. For a squeezed state [54], the Hamiltonian consists of terms quadratic in the creation and the annihilation operator. The Gaussian unitary corresponding to the one mode squeezing operator is

$$S(r) = \exp [r (a^2 - (a^\dagger)^2)] .$$

Here we assume $r \in \mathbb{R}$ for the sake of convenience. The Bogoliubov transformation of the annihilation and creation operator based on the squeezing operator reads:

$$\begin{aligned} S^\dagger(r) a S(r) &= a \cosh r - a^\dagger \sinh r, \\ S^\dagger(r) a^\dagger S(r) &= a^\dagger \cosh r - a \sinh r, \end{aligned}$$

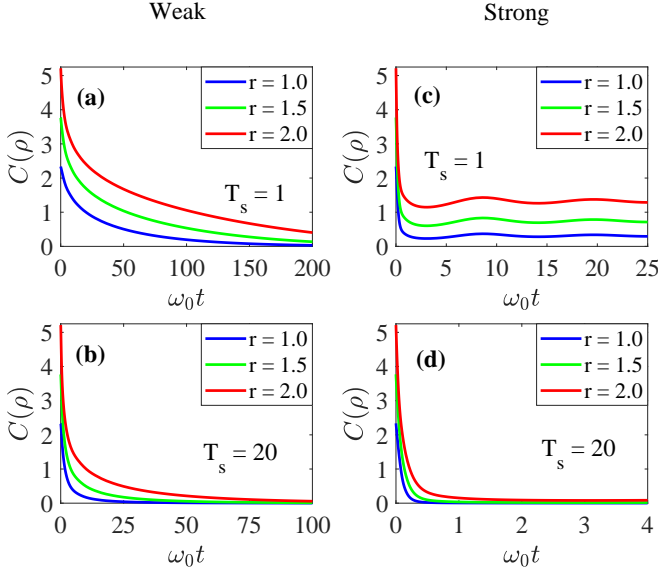


Figure 4: A squeezed mode in contact with a Ohmic bath is studied for weakly interacting systems ($\eta = 0.01 \eta_c$) for (a) $T_s = 1$ and $T_s = 20$ and also for strongly coupled systems ($\eta = 2.0 \eta_c$) for (a) $T_s = 1$ and $T_s = 20$. The cut-off frequency used is $\omega_c = 5.0 \omega_0$.

When this squeezing operator is applied to a vacuum state we can generate a squeezed vacuum state

$$|0, r\rangle = S(r)|0\rangle = \frac{1}{\sqrt{\cosh r}} \sum_{n=0}^{\infty} \frac{\sqrt{(2n)!}}{2^n n!} \tanh^n r |2n\rangle.$$

In this state, the variance of one of the quadrature operator is below the quantum shot noise and hence it is called a squeezed state. To compensate the squeezing in one quadrature, there is an antisqueezing in the other quadrature. The dynamics of quantum coherence of the single mode squeezed state is presented in this section, for the spectral density Eq. (3.20), considering the Ohmic, sub-Ohmic and the super-Ohmic conditions.

Ohmic bath ($s=1$):

The Ohmic bath has a spectral density $J(\omega) = \eta \omega \exp(-\omega/\omega_c)$ and the dynamics of quantum coherence of a single mode squeezed state is given through the plots in Fig. (4). When the squeezed single mode system is weakly coupled ($\eta = 0.01 \eta_c$) to the environment, the coherence evolution is shown through Fig. 4(a) and Fig. 4(b) for the high and the low temperature limits respectively. We do not observe non-Markovian effects in both the limits. But the coherence falls faster in the high temperature limit due to temperature dependent decoherence effects. Under the conditions when the system is strongly coupled to the environment ($\eta = 2.0 \eta_c$), the coherence evolution is shown in Fig. 4 (c) and Fig. 4 (d) respectively. We observe a very small non-Markovian effects in the low temperature limit. It is absent in the high temperature limit due to the thermal decoherence effects.

Sub-Ohmic bath ($s=1/2$):

For a sub-Ohmic bath with spectral density, $J(\omega) =$

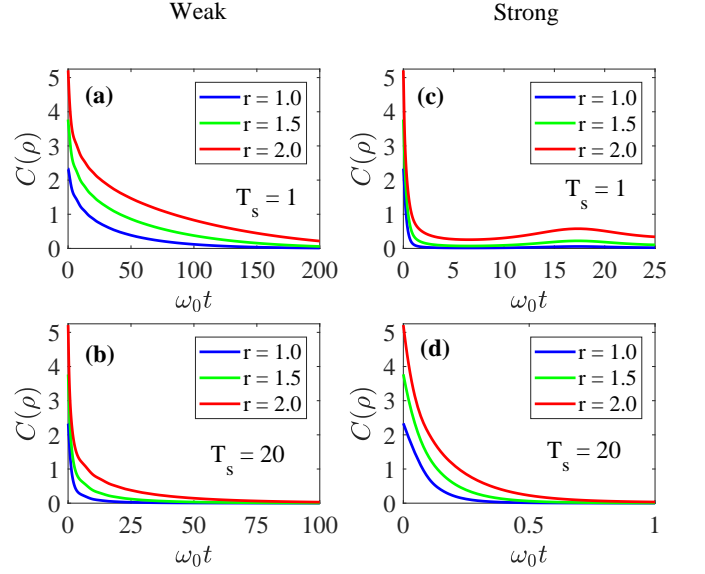


Figure 5: The transient dynamics of coherence for a single squeezed mode in contact with a sub-Ohmic bath is studied for weakly interacting systems ($\eta = 0.01 \eta_c$) for (a) $T_s = 1$ and (b) $T_s = 20$ and strongly interacting systems ($\eta = 2.0 \eta_c$) (c) $T_s = 1$ and (d) $T_s = 20$ and using a cut-off frequency of $\omega_c = 5.0 \omega_0$.

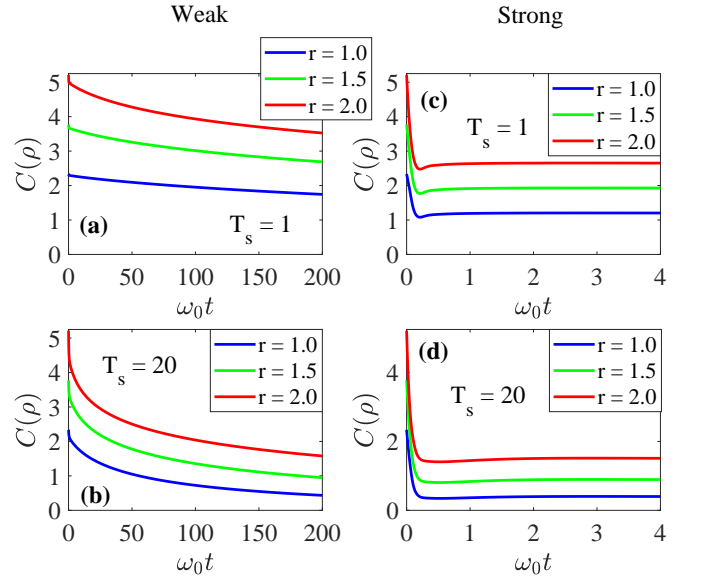


Figure 6: For a squeezed mode in contact with a super-Ohmic bath, the coherence dynamics is studied for weakly interacting systems ($\eta = 0.01 \eta_c$) for (a) $T_s = 1$ and (b) $T_s = 20$ and strongly coupled systems ($\eta = 2.0 \eta_c$) (c) $T_s = 1$ and (d) $T_s = 20$. The cut-off frequency used is $\omega_c = 5.0 \omega_0$.

$\eta \sqrt{\omega \omega_c} \exp(-\omega/\omega_c)$, the coherence dynamics of the single mode squeezed state is shown via the plots in Fig. 5 (a) - (d). In Fig. 5 (a) and 5(b), the system is analyzed when it is weakly coupled to the bath ($\eta = 0.01 \eta_c$). Here we see that at high temperature the coherence falls faster due to thermal decoherence. The strong coupling

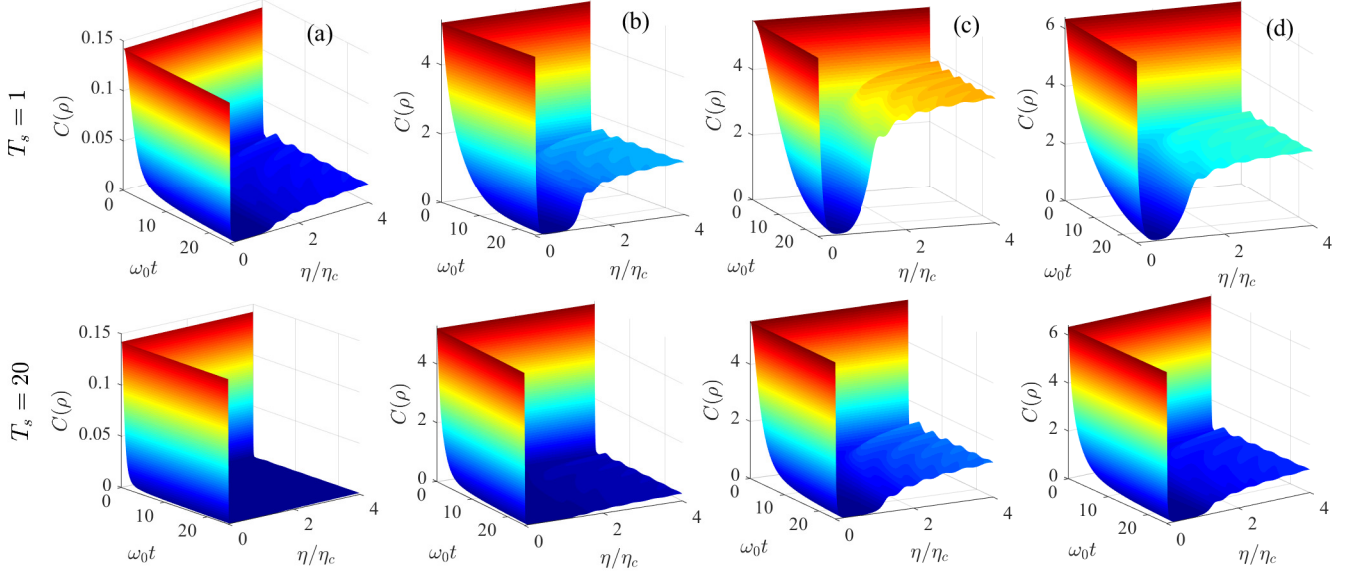


Figure 7: The temporal evolution of the quantum coherence (C) as a function of time ($\omega_0 t$) and coupling strength (η/η_c) is given for the displaced squeezed state in contact with an Ohmic bath. The plot is divided into four columns as (a) $\alpha = 0.1, r = 0.1$, (b) $\alpha = 0.1, r = 2.0$ (c) $\alpha = 4.0, r = 0.1$ and (d) $\alpha = 4.0, r = 2.0$. In each column there are two plots one for $T_s = 1$ and $T_s = 20$. The cut-off frequency used is $\omega_c = 5.0 \omega_0$.

effects ($\eta = 2.0 \eta_c$) are analyzed in the plots 5(c) and 5(d) respectively. In the low temperature limit, there is a small non-Markovian effect, but in the high temperature limit, there is no environmental back action. Overall, we find that coherence falls faster with increase in temperature.

VI. QUANTUM COHERENCE EVOLUTION OF DISPLACED SQUEEZED STATES

A displaced squeezed [55] state has a general form as given below:

$$|\alpha, r\rangle = D(\alpha)S(r)|0\rangle,$$

where $|0\rangle$ is the vacuum state and $D(\alpha)$ and $S(r)$ are the displacement and squeezing operators given below:

$$D(\alpha) = \exp(\alpha a^\dagger - \alpha^* a); \quad S(r) = \exp(ra^2 - r(a^\dagger)^2).$$

Here $\alpha \in \mathbb{C}$ and $r \in \mathbb{R}$ are the relevant parameters. In this state, we investigate the transient dynamics of quantum coherence for different values of the displacement parameter α and the squeezing parameter r . The single mode displaced squeezed state is examined for the spectral density Eq. (3.20), considering the Ohmic, sub-Ohmic and the super-Ohmic conditions.

Ohmic bath ($s=1$) :

Ohmic bath has a spectral density $J(\omega) = \eta\omega \exp(-\omega/\omega_c)$ and the coherence dynamics of the single mode displaced squeezed state for this spectrum is given through the 3D plots in Fig. 7. The coherence $C(\rho)$ being the vertical axis and the parameters $\omega_0 t$ and η/η_c along the orthogonal horizontal axes. The figure is split into four columns labelled from (a) to (d) corresponding to the four different states of the displaced squeezed states. The first row gives the plots in the low temperature limit ($T_s = 1$) and the second row the high temperature regime ($T_s = 20$).

In the first column i.e., Fig. 7 (a), we present the dynamics for the parameter values of ($\alpha = 0.1, r = 0.1$). Both in

Super-Ohmic bath ($s=3$):

To study the effects of a super-Ohmic environment, we consider a bath with a spectral density $J(\omega) = \eta\omega_c(\omega/\omega_c)^3 \exp(-\omega/\omega_c)$. The plots in Fig. 6 (a) - (d) show the dynamics of the quantum coherence of the squeezed single mode state. The change of coherence with time, when the system is weakly coupled to the bath ($\eta = 0.01 \eta_c$) is shown in Fig. 6 (a) and (b). The coherence falls monotonically in the weak coupling limit and the rate of fall of coherence increases with increase in the temperature. In the strong coupling limit i.e., when ($\eta = 2.0 \eta_c$), the coherence initially decreases but saturates at a finite value, a phenomenon known as coherence freezing. The rate of fall of coherence and the saturation value of coherence is dependent on the temperature and for higher temperature the coherence saturates at a lower value. In general we find that the amount of coherence is directly proportional to the squeezing parameter r , under all the environmental conditions.

the high and low temperature limit, the coherence falls monotonically to zero in a very fast manner which can be referred to as coherence sudden death in analogy with the sudden death of entanglement. In the low temperature limit the coherence revives and saturates at a finite value, which does not happen when the temperature is high. After revival in the low temperature limit, the coherence attains saturation and here it shows a non-Markovian feature that survives for a long time. When the squeezing is increased to high values ($\alpha = 0.1, r = 2.0$), the coherence behavior is shown in Fig. 7 (b). Here we again find a coherence sudden death in both the low and high temperature limits. When the displacement values are higher, the coherence is shown in Fig. 7 (c) and 7 (d) for the values ($\alpha = 4.0, r = 0.1$) and ($\alpha = 4.0, r = 2.0$) respectively. The system shows coherence sudden death after which there is a coherence revival and saturation in this limit. The system exhibits non-Markovian behavior for the parameters after the revival. From all the plots Fig. 7 (a) to (d) we can see that the saturation value is higher when ($\alpha = 4.0, r = 0.1$) and on increasing the squeezing parameter it decreases as can be seen from Fig 7 (d) corresponding to the parameter values ($\alpha = 4.0, r = 2.0$).

Sub-Ohmic bath ($s=1/2$):

The single displaced squeezed mode on being affected by a sub-Ohmic bath is given through the plots in Fig. 8. The corresponding spectral density is $J(\omega) = \eta\sqrt{\omega\omega_c}\exp(-\omega/\omega_c)$. The 3D plots describing the variation of coherence given as a set of plots, where the first row represents the low temperature regime ($kT = 1$) and the second row representing the high temperature regime ($kT = 20$). We label the columns from (a) to (d) in the plots.

For the parameter values of ($\alpha = 0.1, r = 0.1$) and ($\alpha = 0.1, r = 2.0$), the coherence dynamics is given in Fig. 8 (a) and (b) respectively. Here in the low temperature limit we observe both coherence sudden death and coherence revival and also a non-Markovian effect in the coherence obtained after the revival. Meanwhile in the high temperature limit, we observe only coherence sudden death and there is no revival. In the regimes ($\alpha = 4.0, r = 0.1$) and ($\alpha = 4.0, r = 2.0$) we see the coherence again decaying within a short interval of time as shown through the plots in Fig. 8 (c) and (d) respectively. The coherence sudden death and the coherence revival is observed both in the low and high temperature limit. Also the non-Markovian effects are clearly seen in these plots. In the sub-Ohmic limit, we see coherence revivals only in the high α region.

Super-Ohmic bath ($s=3$):

The quantum coherence dynamics of the single displaced squeezed mode, when it is exposed to a super-Ohmic environment is given here. The spectral density used for this computation is $J(\omega) = \eta\omega_c(\omega/\omega_c)^3\exp(-\omega/\omega_c)$. The results pertaining to this study is given as 3D plots in Fig. 9, with the coherence $C(\rho)$ being along the vertical axis and the parameters $\omega_0 t$ and η/η_c along the orthogonal horizontal axes. The first row represents the low tem-

perature regime ($T_s = 1$) and the second row the high temperature regime ($T_s = 20$) and the columns in the figure are labelled from (a) to (d).

In Fig. 9 (a) and (b) the coherence dynamics is given for parameter values of ($\alpha = 0.1, r = 0.1$) and ($\alpha = 0.1, r = 2.0$) respectively. For the parameter values ($\alpha = 4.0, r = 0.1$) and ($\alpha = 4.0, r = 2.0$), the dynamics is given through the plots in Fig. 9 (c) and (d). From all the plots we observe that the coherence decays monotonically and then attains a saturation value at which the coherence freezes for the rest of the evolution. But the fall of coherence and the value at which the coherence freezes is dependent on the temperature and higher the temperature, lower the saturation value. This is because apart from the loss of coherence due to dissipation, some of the coherence is also lost due to the thermal decoherence. From Fig. 9 (a) we can see that initial coherence is low when both the α and r values are low. On increasing either the displacement parameter α or the squeezing parameter r , we find that the system has a higher amount of initial coherence i.e., coherence at $t = 0$ as shown in Fig. 9 (b) and (c). Further, from these two cases, we also observe that the saturation value is higher when α is higher. Finally in 9 (d) we examine the situation where both the displacement parameter (α) and the squeezing parameter (r) are higher. In this case we find that the initial amount of coherence is comparable to the cases in Fig. 9 (b) and (c), but the fall of coherence and the saturation value more closely resembles the case in Fig. 9 (c), where ($\alpha = 4.0, r = 0.1$). An increase in either the displacement parameter or the squeezing parameter increases the quantum coherence in the system.

VII. MARKOVIAN TO NON-MARKOVIAN CROSSOVER

The present work considers a Gaussian state in contact with an external non-Markovian environment. When we consider a Ohmic or sub-Ohmic bath coupled to the system, we initially observe a Markovian evolution for the coherent state, squeezed state and displaced squeezed state. Depending on whether the coupling is weak or strong, the dynamics continues to remain either Markovian or switches over to non-Markovian behavior. In this current section we examine the crossover behavior in the dynamics of a displaced squeezed state.

Let us consider the evolution of a displaced squeezed state with the parameter values of $\alpha = 4.0$ and $r = 0.1$. When the coupling between the bath and the system is weak, we observe that the dynamics of the system is completely Markovian where the system experiences either a death of coherence or coherence freezing. In this case, the correlation time of the bath is much shorter than the system evolution time. The irreversible loss of information occurs, because the bath states are restored very quickly and so any information received from the state is lost. For systems which have a stronger coupling

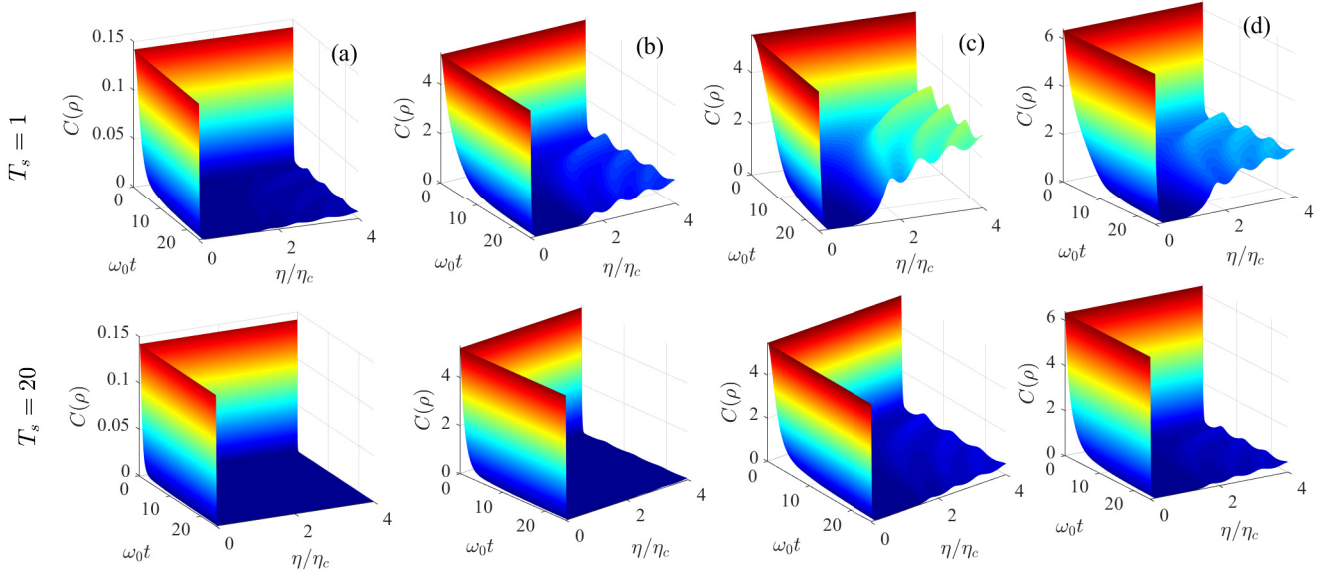


Figure 8: The coherence dynamics of a displaced squeezed mode is shown in the figure above as a function of time $\omega_0 t$, and η/η_c when it is in contact with a sub-Ohmic bath. The plot is divided into four columns (a) $\alpha = 0.1, r = 0.1$, (b) $\alpha = 0.1, r = 2.0$, (c) $\alpha = 4.0, r = 0.1$, and (d) $\alpha = 4.0, r = 2.0$. In each column there are two plots for $T_s = 1$ and $T_s = 20$. The cut-off frequency used is $\omega_c = 5.0 \omega_0$.

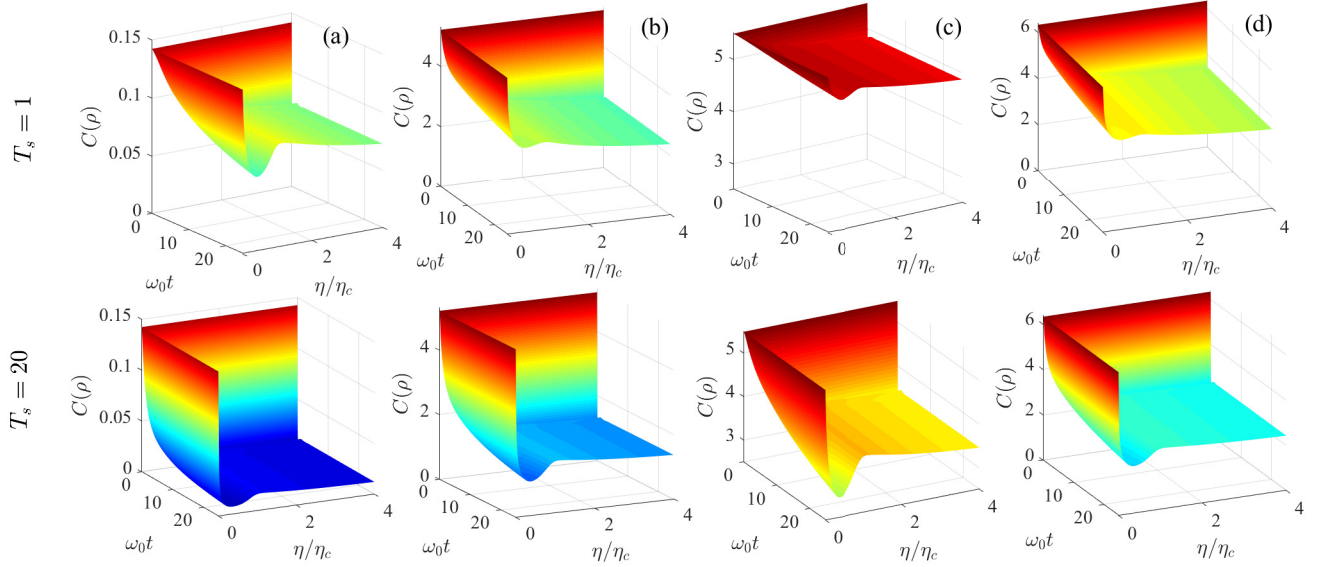


Figure 9: The time evolution of coherence of a displaced squeezed mode in contact with a super-Ohmic bath is shown in the figure above as a function of $\omega_0 t$, and η/η_c . There are four columns in the plot (a) $\alpha = 0.1, r = 0.1$, (b) $\alpha = 0.1, r = 2.0$, (c) $\alpha = 4.0, r = 0.1$, and (d) $\alpha = 4.0, r = 2.0$. In each column there are two plots for $T_s = 1$ and $T_s = 20$. The cut-off frequency used is $\omega_c = 5.0 \omega_0$.

with the bath, the initial coherence decay is Markovian and then there is a sudden switch where the dynamics becomes non-Markovian. In the non-Markovian phase there is a back flow of information from the environment to the system. To check this behaviour, we look at Fig. 10, the 3D plots of $\frac{dC}{d\eta_s}$ Vs η_s Vs $\omega_0 t$ in both the low

temperature ($T_s = 1$) and the high temperature ($T_s = 20$) limits. In Fig. 10 (a), the plot shows $dC/d\eta_s$ for the Ohmic spectrum in the low temperature limit. Here we find that initially, the slope is $-ve$ and monotonic implying a Markovian nature. Increasing the coupling strength, we observe that the slope changes from $-ve$ to $+ve$ indicating

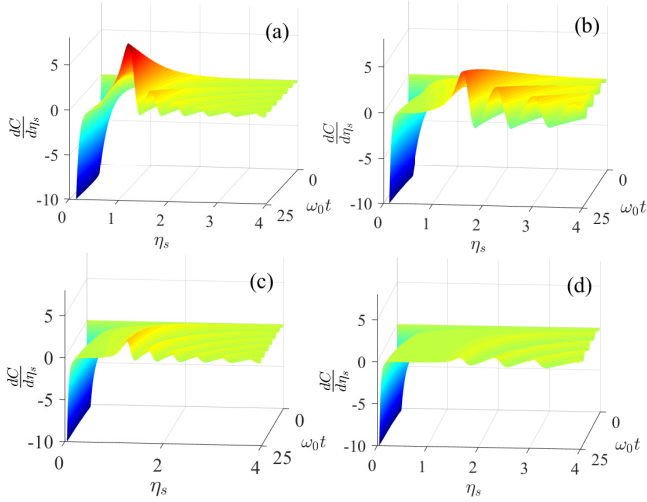


Figure 10: The 3-D plots $\frac{dC}{d\eta_s}$ Vs η_s Vs $\omega_0 t$ for the squeezed coherent state with parameters $\alpha = 4.0$, $r = 0.1$ is given above. In Fig. (a) and (c) we study the low temperature ($T_s = 1$) and the high temperature limit ($T_s = 20$) when the state is in contact with an Ohmic bath. The low temperature ($T_s = 1$) and high temperature limit ($T_s = 20$) is shown in Figs. (b) and (d) respectively, when the state is exposed to a sub-Ohmic bath. The cut-off frequency used is $\omega_c = 5.0 \omega_0$.

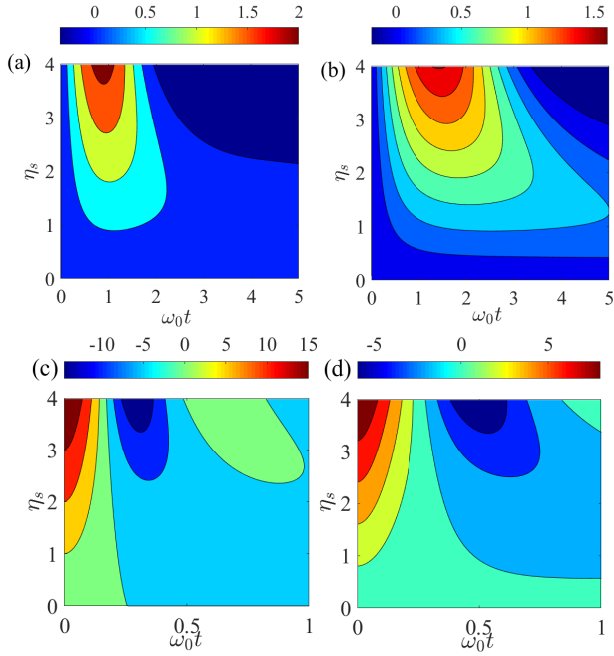


Figure 11: The dissipation coefficient $\gamma(t)$ is calculated from the exact solution of $u(t)$. We present here the contour plot of the dissipation coefficient $\gamma(t)$ and its time derivative $d\gamma/dt$ with varying time and coupling strength. In Fig. (a) and (b) we show the transient behavior of $\gamma(t)$ for Ohmic ($s = 1$) and sub-Ohmic ($s = 1/2$) bath spectrum respectively. We next plot the time derivative $d\gamma/dt$ with varying time and coupling strength when the system is in contact with an Ohmic bath (c) and sub-Ohmic bath (d) respectively. The cut-off frequency $\omega_c = 5.0\omega_0$.

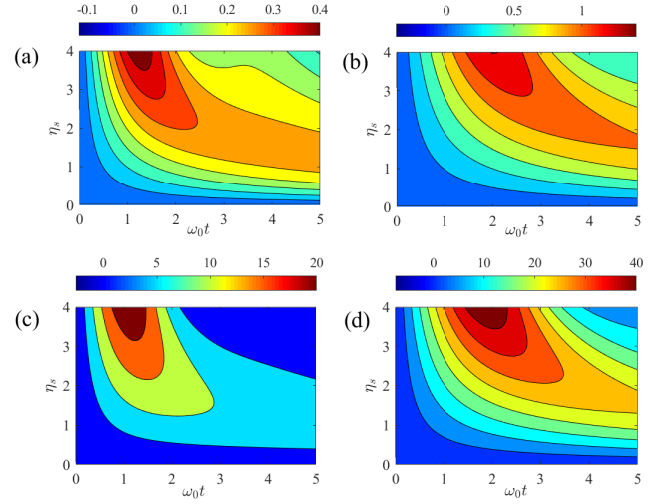


Figure 12: The fluctuation coefficient $\tilde{\gamma}(t)$ is calculated from the exact solution of $u(t)$ and $v(t)$. We present here the contour plot of the fluctuation coefficient $\tilde{\gamma}(t)$ for Ohmic ($s = 1$) spectrum in the low temperature (a) $T_s = 1$ and in the higher temperature (c) $T_s = 20$ respectively. We next show the contour plot of fluctuation coefficient $\tilde{\gamma}(t)$ for sub-Ohmic ($s = 1/2$) spectrum in the low temperature (b) $T_s = 1$ and in the high temperature (d) $T_s = 20$. The cut-off frequency in all the cases $\omega_c = 5.0\omega_0$.

a change from Markovian to non-Markovian behavior. For the Ohmic bath in the low temperature regime this crossover in the behavior of dynamics is very abrupt and this sudden change is reminiscent of a phase transition. In the initial phase we observe $\tau_b \ll \tau_s$, where τ_b is the relaxation time of the bath and τ_s is the evolution time of the system. After the crossover (i.e., transition) the time scales are related as $\tau_b \approx \tau_s$ indicative of a new phase. In the low temperature limit ($T_s = 1$), the sub-Ohmic regime is described in Fig. 10 (b). Here there is a region where the coherence remains constant before the transition to the non-Markovian evolution. The high temperature ($T_s = 20$) case of the 3D plots are shown in Fig. 10 (c) and (d) for the Ohmic and sub-Ohmic baths respectively. From the plots we can observe that transition region between the Markovian and non-Markovian regimes is more pronounced. Also the non-Markovian effect is decreased indicating a lesser amount of environmental back flow of coherence. This reduced amount of back flow is due to the decoherence caused by thermal effects.

The dynamical behavior of the continuous variable system can also be studied using a quantum master equation. The crossover between Markovian and non-Markovian can be perceived from the changing behavior of the decay rates in the master equation. The total density matrix ρ_{tot} describing the continuous variable system and environment has a dynamics governed by the quantum evolution operator $\rho_{tot}(t) = \exp(-\frac{i}{\hbar}Ht)\rho_{tot}(0)\exp(\frac{i}{\hbar}Ht)$. The initial state of the system is considered to be $\rho_{tot}(0) = \rho_s(0) \otimes \rho_E(0)$, where $\rho_E(0) = \exp(-\beta H_E)/(\text{Tr} \exp(-\beta H_E))$ as proposed in [56, 57]. Tracing over the environmental de-

degrees of freedom we can get the reduced density matrix of the system. The master equation for the reduced density matrix reads:

$$\begin{aligned} \frac{d\rho(t)}{dt} = & -i\omega'_0(t)[a^\dagger a, \rho(t)] \\ & + \gamma(t)[2a\rho(t)a^\dagger - a^\dagger a\rho(t) - \rho(t)a^\dagger a] \\ & + \tilde{\gamma}(t)[a\rho(t)a^\dagger + a^\dagger \rho(t)a - a^\dagger a\rho(t) - \rho(t)aa^\dagger] \end{aligned} \quad (7.1)$$

where the coefficients are

$$\begin{aligned} \omega'_0(t) = \text{Im} \left[\frac{\dot{u}(t)}{u(t)} \right], \quad \gamma(t) = -\text{Re} \left[\frac{\dot{u}(t)}{u(t)} \right] \\ \tilde{\gamma}(t) = \dot{v}(t) - 2v(t)\text{Re} \left[\frac{\dot{u}(t)}{u(t)} \right]. \end{aligned}$$

Here $\omega'_0(t)$ is the renormalized frequency of the single mode system and $\gamma(t)$ and $\tilde{\gamma}(t)$ are the dissipation and fluctuation coefficients. In Fig. 11 (a) and (b), we present a contour plot of the dissipation coefficient $\gamma(t)$ varying with time and coupling strength. The Ohmic case is described through the plot in 11(a), where in the weak coupling limit $\eta_s \leq 1$ we find that the dissipation is almost a constant throughout the entire evolution. For the strong coupling regime $\eta_s \geq 1$, the dissipation rate $\gamma(t)$ increases initially and then decreases. This change in the direction of the decay rate with time, indicates a backflow of information from the environment to the system. A similar behavior of the dissipation constant $\gamma(t)$ is observed in the sub-Ohmic case as shown in 11(b). The reverse flow of information is more transparent from the contour plot of the slope of $\gamma(t)$. We show contour plot of the time derivative of the decay rate ($d\gamma/dt$) for the Ohmic case in Fig. 11 (c) and sub-Ohmic case in Fig. 11 (d). From the plot we observe that the slope of the dissipation coefficient $\gamma(t)$, transitions from being positive to negative. This is indicative of a crossover from the Markovian to a non-Markovian regime.

Next, we study the variation of the fluctuation coefficient namely $\tilde{\gamma}(t)$ in Fig. 12. We show the contour plot of fluctuation coefficient for Ohmic spectrum in the low temperature limit ($T_s = 1$) in Fig. 12 (a) and for the high temperature limit ($T_s = 20$) in Fig. 12 (c). In the strong coupling regime ($\eta_s \geq 1$), the fluctuation coefficient $\tilde{\gamma}(t)$ rises initially and then starts decreasing with time. This changing behavior of $\tilde{\gamma}(t)$ indicates the environmental back action in the strong coupling regime. The contour plot of fluctuation coefficient for sub-Ohmic spectrum in the low temperature ($T_s = 1$) is shown in Fig. 12 (b). For the high temperature limit ($T_s = 20$) is given in Fig. 12 (d). We observe a similar dynamical crossover of $\tilde{\gamma}(t)$ for the sub-Ohmic spectral density as well. Hence the environmental back flow of information [58–60] i.e., the non-Markovian behavior can be obtained from the dynamical behavior of the dissipation and the fluctuation coefficients. The dynamical crossover observed in the coherence dynamics of a single mode state, stands verified by the analysis carried out from the dynamics of the fluctuation and dissipation coefficients of the master equation of the state.

VIII. CONCLUSION

The transient dynamics of quantum coherence of a single mode Gaussian state is analyzed in the open quantum system formalism. For this we consider a non-Markovian environment, which is a collection of infinite bosonic modes of varying frequencies. The entire analysis is carried out in the finite temperature limit with arbitrary system-bath coupling strength. To measure the quantum coherence we use the relative entropy measure which estimates the distance to the thermal state. Hence the quantum coherence can be completely characterized by the determinant of the covariance matrix and the average of the number operator of the Gaussian states. We solve the quantum Langevin equation for the bosonic mode operators to obtain the time evolved covariance matrix elements. The time evolution of the field operators are determined by the two basic nonequilibrium Green's functions namely $u(t)$ and $v(t)$.

The time dynamics of quantum coherence is studied for three distinct experimentally realizable Gaussian states. The investigations have been carried out under three different environmental spectral densities *viz* Ohmic, sub-Ohmic and super-Ohmic spectral densities. When the system interacts weakly with the environment, the quantum coherence decreases monotonically with time. The coherence decay rate is relatively lower for the super-Ohmic bath when compared with the Ohmic and the sub-Ohmic baths. Also the rate of decay increases with the temperature. In general we observe a coherence death for the Ohmic and the sub-Ohmic baths in the short time limit. For the super-Ohmic bath we observe coherence freezing which is a saturation of coherence at a finite value. In the strong coupling regime, the coherence decreases initially and then starts increasing resulting in a revival of coherence for the Ohmic and the sub-Ohmic baths. This is followed by a stabilization of coherence with an oscillatory phase. This oscillatory behavior is due to the environmental backaction which is a feature of non-Markovian dynamics in the system. Hence in our study we observe a transition or crossover from the Markovian dynamics to the non-Markovian dynamics. The non-Markovian memory effect helps us to restore quantum resources in the strong coupling limit. The rate at which the crossover in the dynamics occurs depends on the parameters of the Gaussian state as well as on the environmental parameters. To verify the existence of the crossover we study the dynamical behavior of the quantum system using a master equation approach. Here we compute the dissipation and fluctuation coefficients in the master equation of the reduced density matrix. Throughout the evolution, the dissipation rate is almost a constant in the weak coupling limit. In the strong coupling limit, the dissipation rate increases initially and then decreases, which implies a Markovian to non-Markovian transition. A plot of the time derivative of the decay rate shows that the slope of the dissipation coefficient changes from being positive to negative. This is a clear indication of the crossover

from the Markovian to the non-Markovian dynamics. This crossover feature is also verified from the dynamics of the fluctuation coefficient. Thus we find that the quantum system has both Markovian and non-Markovian behavior at different times and there is a dynamical crossover from the Markovian to the non-Markovian regime. This change from Markovian to non-Markovian regime is not a gradual change. Instead it is either a sudden change or there is a time period between the Markovian and non-Markovian regimes, where there is no dynamical change. This raises an important question as to whether this dynamical change can be considered as some kind of phase transition between two different regimes with totally different relaxation time scales. While the results seems to point towards such a conclusion, a more detailed study from the point of view of quantum phase transitions is needed to confirm and validate this, and such a study will form the scope of our future works. A similar observation on an abrupt change from Markovian to non-Markovian dynamics has also been made in Ref. [61]. Here the authors

study a single qubit system in contact with a single qubit environment. In our work we consider a single mode Gaussian state in contact with a structured bosonic reservoir with a collection of infinite modes to describe a general non-Markovian environment. The investigations carried out in the present work can be experimentally verified by measuring the quantum coherence of Gaussian systems [62–65].

ACKNOWLEDGEMENTS

Md. Manirul Ali was supported in part by the Centre for Quantum Science and Technology, Chennai Institute of Technology, India, vide funding number CIT/CQST/2021/RD-007. Chandrashekar Radhakrishnan was supported in part by a seed grant from IIT Madras to the Centre for Quantum Information, Communication and Computing.

-
- [1] R. J. Glauber, Coherent and incoherent states of the radiation field, *Physical Review* **131**, 2766 (1963).
 - [2] T. Baumgratz, M. Cramer, and M. B. Plenio, Quantifying coherence, *Physical review letters* **113**, 140401 (2014).
 - [3] A. Winter and D. Yang, Operational resource theory of coherence, *Physical Review Letters* **116**, 120404 (2016), 1506.07975.
 - [4] F. G. Brandão and G. Gour, Reversible framework for quantum resource theories, *Physical Review Letters* **115**, 070503 (2015).
 - [5] A. Streltsov, G. Adesso, and M. B. Plenio, Colloquium: Quantum coherence as a resource, *Reviews of Modern Physics* **89**, 041003 (2017).
 - [6] E. Chitambar and G. Gour, Quantum resource theories, *Reviews of Modern Physics* **91**, 025001 (2019).
 - [7] E. Chitambar and M.-H. Hsieh, Relating the resource theories of entanglement and quantum coherence, *Physical Review Letters* **117**, 020402 (2016).
 - [8] J. Wang, Z. Tian, J. Jing, and H. Fan, Irreversible degradation of quantum coherence under relativistic motion, *Physical Review A* **93**, 062105 (2016), 1601.03238.
 - [9] J. He, Z.-Y. Ding, J.-D. Shi, and T. Wu, Multipartite quantum coherence and distribution under the unruh effect, *Annalen der Physik* **530**, 1800167 (2018).
 - [10] S. Bhattacharya, S. Banerjee, and A. K. Pati, Evolution of coherence and non-classicality under global environmental interaction, *Quantum Information Processing* **17**, 1 (2018).
 - [11] C. Radhakrishnan, P.-W. Chen, S. Jambulingam, T. Byrnes, and M. M. Ali, Time dynamics of quantum coherence and monogamy in a non-markovian environment, *Scientific reports* **9**, 1 (2019).
 - [12] C. Radhakrishnan, Z. Lü, J. Jing, and T. Byrnes, Dynamics of quantum coherence in a spin-star system: Bipartite initial state and coherence distribution, *Physical Review A* **100**, 042333 (2019).
 - [13] H. Cao, C. Radhakrishnan, M. Su, M. M. Ali, C. Zhang, Y.-F. Huang, T. Byrnes, C.-F. Li, and G.-C. Guo, Fragility of quantum correlations and coherence in a multipartite photonic system, *Physical Review A* **102**, 012403 (2020).
 - [14] S. L. Braunstein and P. Van Loock, Quantum information with continuous variables, *Reviews of modern physics* **77**, 513 (2005).
 - [15] G. Adesso, S. Ragy, and A. R. Lee, Continuous variable quantum information: Gaussian states and beyond, *Open Systems & Information Dynamics* **21**, 1440001 (2014).
 - [16] C. Weedbrook, S. Pirandola, R. García-Patrón, N. J. Cerf, T. C. Ralph, J. H. Shapiro, and S. Lloyd, Gaussian quantum information, *Reviews of Modern Physics* **84**, 621 (2012).
 - [17] X.-B. Wang, T. Hiroshima, A. Tomita, and M. Hayashi, Quantum information with gaussian states, *Physics reports* **448**, 1 (2007).
 - [18] S. Olivares, Quantum optics in the phase space, *The European Physical Journal Special Topics* **203**, 3 (2012).
 - [19] J. Xu, Quantifying coherence of gaussian states, *Physical Review A* **93**, 032111 (2016).
 - [20] H.-P. Breuer, E.-M. Laine, J. Piilo, and B. Vacchini, Colloquium: Non-markovian dynamics in open quantum systems, *Reviews of Modern Physics* **88**, 021002 (2016).
 - [21] I. De Vega and D. Alonso, Dynamics of non-markovian open quantum systems, *Reviews of Modern Physics* **89**, 015001 (2017).
 - [22] A. Shnirman, Y. Makhlin, and G. Schön, Noise and decoherence in quantum two-level systems, in *Condensation And Coherence In Condensed Matter* (World Scientific, 2003) pp. 147–154.
 - [23] O. Astafiev, Y. A. Pashkin, Y. Nakamura, T. Yamamoto, and J.-S. Tsai, Temperature square dependence of the low frequency $1/f$ charge noise in the josephson junction qubits, *Physical review letters* **96**, 137001 (2006).
 - [24] F. Yoshihara, K. Harrabi, A. Niskanen, Y. Nakamura, and J. S. Tsai, Decoherence of flux qubits due to $1/f$ flux noise, *Physical review letters* **97**, 167001 (2006).
 - [25] N.-H. Tong and M. Vojta, Signatures of a noise-induced quantum phase transition in a mesoscopic metal ring,

- Physical review letters **97**, 016802 (2006).
- [26] K. Kakuyanagi, T. Meno, S. Saito, H. Nakano, K. Semba, H. Takayanagi, F. Deppe, and A. Shnirman, Dephasing of a superconducting flux qubit, *Physical review letters* **98**, 047004 (2007).
 - [27] C. Seoanez, F. Guinea, and A. C. Neto, Dissipation due to two-level systems in nano-mechanical devices, *EPL (Europhysics Letters)* **78**, 60002 (2007).
 - [28] P. Ribeiro and V. R. Vieira, Non-markovian effects in electronic and spin transport, *Physical Review B* **92**, 100302 (2015).
 - [29] P. B. Vyas, M. L. Van de Put, and M. V. Fischetti, Master-equation study of quantum transport in realistic semiconductor devices including electron-phonon and surface-roughness scattering, *Physical Review Applied* **13**, 014067 (2020).
 - [30] T. Yu and J. Eberly, Finite-time disentanglement via spontaneous emission, *Physical Review Letters* **93**, 140404 (2004).
 - [31] T. Yu and J. Eberly, Sudden death of entanglement: classical noise effects, *Optics Communications* **264**, 393 (2006).
 - [32] T. Yu and J. Eberly, Sudden death of entanglement, *Science* **323**, 598 (2009).
 - [33] B. Bellomo, R. L. Franco, and G. Compagno, Non-markovian effects on the dynamics of entanglement, *Physical Review Letters* **99**, 160502 (2007).
 - [34] X. Deng, Y. Liu, M. Wang, X. Su, and K. Peng, Sudden death and revival of gaussian einstein-podolsky-rosen steering in noisy channels, *npj Quantum Information* **7**, 1 (2021).
 - [35] J.-S. Xu, C.-F. Li, M. Gong, X.-B. Zou, C.-H. Shi, G. Chen, and G.-C. Guo, Experimental demonstration of photonic entanglement collapse and revival, *Physical review letters* **104**, 100502 (2010).
 - [36] L. Mazzola, S. Maniscalco, J. Piilo, K.-A. Suominen, and B. M. Garraway, Sudden death and sudden birth of entanglement in common structured reservoirs, *Physical Review A* **79**, 042302 (2009).
 - [37] K.-L. Liu and H.-S. Goan, Non-markovian entanglement dynamics of quantum continuous variable systems in thermal environments, *Physical Review A* **76**, 022312 (2007).
 - [38] J.-H. An and W.-M. Zhang, Non-markovian entanglement dynamics of noisy continuous-variable quantum channels, *Physical Review A* **76**, 042127 (2007).
 - [39] J. P. Paz and A. J. Roncaglia, Dynamics of the entanglement between two oscillators in the same environment, *Physical review letters* **100**, 220401 (2008).
 - [40] R. Simon, N. Mukunda, and B. Dutta, Quantum-noise matrix for multimode systems: $U(n)$ invariance, squeezing, and normal forms, *Physical Review A* **49**, 1567 (1994).
 - [41] Y.-R. Zhang, L.-H. Shao, Y. Li, and H. Fan, Quantifying coherence in infinite-dimensional systems, *Physical Review A* **93**, 012334 (2016).
 - [42] B. L. Schumaker, Quantum mechanical pure states with gaussian wave functions, *Physics Reports* **135**, 317 (1986).
 - [43] Z. Ding, R. Liu, C. Radhakrishnan, W. Ma, X. Peng, Y. Wang, T. Byrnes, F. Shi, and J. Du, Experimental study of quantum coherence decomposition and trade-off relations in a tripartite system, *npj Quantum Information* **7**, 1 (2021).
 - [44] H.-N. Xiong, W.-M. Zhang, X. Wang, and M.-H. Wu, Exact non-markovian cavity dynamics strongly coupled to a reservoir, *Physical Review A* **82**, 012105 (2010).
 - [45] W.-M. Zhang, P.-Y. Lo, H.-N. Xiong, M. W.-Y. Tu, and F. Nori, General non-markovian dynamics of open quantum systems, *Physical review letters* **109**, 170402 (2012).
 - [46] M. M. Ali, P.-Y. Lo, and W.-M. Zhang, Exact decoherence dynamics of $1/f$ noise, *New Journal of Physics* **16**, 103010 (2014).
 - [47] M. M. Ali, P.-Y. Lo, M. W.-Y. Tu, and W.-M. Zhang, Non-markovianity measure using two-time correlation functions, *Physical Review A* **92**, 062306 (2015).
 - [48] H.-N. Xiong, P.-Y. Lo, W.-M. Zhang, F. Nori, *et al.*, Non-markovian complexity in the quantum-to-classical transition, *Scientific reports* **5**, 1 (2015).
 - [49] P. W. Anderson, Localized magnetic states in metals, *Physical Review* **124**, 41 (1961).
 - [50] U. Fano, Effects of configuration interaction on intensities and phase shifts, *Physical Review* **124**, 1866 (1961).
 - [51] M. M. Ali and W.-M. Zhang, Nonequilibrium transient dynamics of photon statistics, *Physical Review A* **95**, 033830 (2017).
 - [52] M. De Oliveira, M. Moussa, and S. Mizrahi, Continuous pumping and control of a mesoscopic superposition state in a lossy qed cavity, *Physical Review A* **61**, 063809 (2000).
 - [53] A. J. Leggett, S. Chakravarty, A. T. Dorsey, M. P. Fisher, A. Garg, and W. Zwerger, Dynamics of the dissipative two-state system, *Reviews of Modern Physics* **59**, 1 (1987).
 - [54] D. F. Walls, Squeezed states of light, *nature* **306**, 141 (1983).
 - [55] M. Kim, F. De Oliveira, and P. Knight, Properties of squeezed number states and squeezed thermal states, *Physical Review A* **40**, 2494 (1989).
 - [56] R. Feynman and F. Vernon, The theory of a general quantum system interacting with a linear dissipative system, *Annals of Physics* **24**, 118 (1963).
 - [57] A. O. Caldeira and A. J. Leggett, Path integral approach to quantum brownian motion, *Physica A: Statistical mechanics and its Applications* **121**, 587 (1983).
 - [58] H.-P. Breuer, E.-M. Laine, and J. Piilo, Measure for the degree of non-markovian behavior of quantum processes in open systems, *Physical review letters* **103**, 210401 (2009).
 - [59] B.-H. Liu, L. Li, Y.-F. Huang, C.-F. Li, G.-C. Guo, E.-M. Laine, H.-P. Breuer, and J. Piilo, Experimental control of the transition from markovian to non-markovian dynamics of open quantum systems, *Nature Physics* **7**, 931 (2011).
 - [60] D. Chruściński and S. Maniscalco, Degree of non-markovianity of quantum evolution, *Physical review letters* **112**, 120404 (2014).
 - [61] S. Pang, T. Brun, and A. Jordan, Abrupt transition between markovian and non-markovian dynamics in quantum open systems, in *APS March Meeting Abstracts*, Vol. 2018 (2018) pp. S27-008.
 - [62] W. P. Bowen, R. Schnabel, P. K. Lam, and T. C. Ralph, Experimental characterization of continuous-variable entanglement, *Physical review A* **69**, 012304 (2004).
 - [63] A. Furusawa, J. L. Sørensen, S. L. Braunstein, C. A. Fuchs, H. J. Kimble, and E. S. Polzik, Unconditional quantum teleportation, *science* **282**, 706 (1998).
 - [64] H. Yonezawa, T. Aoki, and A. Furusawa, Demonstration of a quantum teleportation network for continuous variables, *Nature* **431**, 430 (2004).
 - [65] J. DiGuglielmo, B. Hage, A. Franzen, J. Fiurášek, and R. Schnabel, Experimental characterization of gaussian quantum-communication channels, *Physical Review A* **76**, 012323 (2007).